

Research Article

# Satellite-Based Validation of Contrail Prediction Models for Sustainable Aviation

**Baddireddi Sree Chandana<sup>1</sup>, Pelleti Nandieswar Reddy<sup>1</sup>, Rithvika Alapati<sup>1</sup>, Sai Aswath Reddy<sup>1</sup>, Radha Doraisamy<sup>1,\*</sup>, Uma Sankari<sup>2</sup>**

<sup>1</sup>Department of Computer Science and Engineering, Amrita School of Computing, Amrita Vishwa Vidyapeetham Bengaluru Campus Kasavanahalli, Carmelaram P.O.

Bengaluru - 560 035 Karnataka, India

<sup>2</sup>Vikram Sarabhai Space Centre, GV6Q+XCG, Veli - Perumathura Rd, Kochuveli, Thiruvananthapuram, Kerala 695022, India

\*e-mail: [d\\_radha@blr.amrita.edu](mailto:d_radha@blr.amrita.edu)

*Submitted: 21/12/2024    Revised: 17/02/2025    Accepted: 20/02/2025    Published online: 26/02/2025*

**Abstract:** The aviation industry significantly contributes to global warming through the formation of contrails, which trap heat in the atmosphere and exacerbate climate change. To mitigate this effect, sophisticated models have been developed to predict contrail formation and its associated warming effects, but these require empirical validation for accuracy. This project leverages satellite imagery to validate contrail prediction models, enabling effective contrail avoidance strategies for airlines. U-Net variants, a convolutional neural network architecture, is utilized for image segmentation to identify contrails in satellite imagery. By optimizing the threshold for the softmax layer, contrail detection accuracy, and validating model predictions with real-world data had been enhanced. This enables pilots to minimize contrail formation during flights, aiming to reduce the aviation industry's environmental impact. The research offers a scalable and cost-effective solution for enhancing aviation sustainability and aligns with global efforts to combat climate change.

**Keywords:** *Contrails; U-Net; Image Segmentation; Satellite Imagery; Climate Change; Contrail Prediction Models*

## I. INTRODUCTION

The aviation industry has long been recognized as a significant contributor to global warming, primarily due to the formation of contrails – those line-shaped clouds of ice crystals emitted from aircraft engine exhaust. These contrails have been identified as a key player in climate change dynamics, exacerbating the environmental impact of air travel by trapping heat in the atmosphere. As concerns over climate change intensify, it becomes imperative for the aviation sector to address its environmental footprint.

Contrails, which are essentially artificial clouds, are formed whenever hot, moist exhaust from aircraft engines mixes with cold air at high altitudes. They not only contribute to the visual pollution of the skies but also play a crucial role in altering the Earth's radiation balance, leading to increased warming of the atmosphere. This phenomenon is particularly concerning given the exponential growth of air travel worldwide, with projections

indicating continued expansion in the coming decades. Recognizing the urgency of mitigating the aviation industry's impact on climate change, researchers have devoted significant efforts to understanding and predicting contrail formation. Sophisticated models have been developed to simulate the complex interactions between aircraft emissions, atmospheric conditions, and contrail formation processes. These models serve as valuable tools for assessing the environmental impact of air travel and devising strategies to minimize it. However, despite advancements in modelling techniques, there remains a critical need for empirical validation to enhance the accuracy and reliability of contrail prediction models. While laboratory experiments and field measurements provide valuable insights, they are often limited in scale and scope. Moreover, conducting extensive observations in the atmosphere poses logistical challenges and may not capture the full complexity of contrail formation dynamics. To address this gap, this project proposes leveraging satellite imagery as

a complementary approach to validate contrail prediction models. Satellites offer a unique vantage point from which to observe contrail formation on a global scale, providing comprehensive coverage of flight paths and atmospheric conditions. By correlating model predictions with real-world observations obtained from satellite imagery, researchers can validate and refine their understanding of contrail formation processes.

The integration of satellite data into contrail prediction models holds promise for enhancing the accuracy of forecasts and improving the effectiveness of contrail avoidance strategies. Armed with validated models, airlines can empower pilots to make informed decisions during flight planning and operations, taking into account factors such as optimal altitude, route selection, and engine settings to minimize contrail formation. By doing so, the aviation industry can mitigate its contribution to climate change while ensuring the sustainability of air travel. In alignment with global efforts to combat climate change, this research aims to provide a scalable and cost-effective solution for reducing the environmental impact of the aviation sector. By leveraging satellite imagery to validate contrail prediction models, this project seeks to enable more informed decision-making and promote sustainable practices within the aviation industry. Through collaborative efforts between researchers, policymakers, and industry stakeholders, it is aimed to work towards a future where air travel is both efficient and environmentally responsible.

## **II. RELATED WORK**

Contrails, or condensation trails, form behind aircraft and significantly contribute to aviation-induced climate change. The mitigation of their impact through contrail avoidance strategies is considered a cost-efficient method to reduce aviation's climate footprint. The introduction of the Open Contrails dataset aims to facilitate the development and evaluation of contrail detection models. This dataset, comprising manually labelled imagery from the GOES-16 Advanced Baseline Imager (ABI), is designed to train models capable of identifying contrails with high accuracy [1]. A proposed contrail detection model incorporates temporal context, enhancing detection accuracy by integrating temporal information into CNN(convolution neural network)-based models. This approach shows promise for better understanding contrail dynamics. The study also suggests leveraging self-supervised and semi-supervised learning techniques to further improve model performance. Expanding the research to include data from geostationary satellites like Himawari-8 and Meteosat-11 could extend coverage, especially over Europe and the Asia-Pacific region, highlighting the importance of

satellite data and CNN models in addressing aviation-induced climate change [1].

A comprehensive study focuses on the detection, tracking, and matching of linear contrails using geostationary satellite infrared images, weather data, and air traffic data. The primary objective is to create a dataset that captures the complete lifecycle of contrails and identifies the aircraft responsible for their formation. This innovative methodology simultaneously addresses tracking and identification challenges, providing a holistic and integrated approach to contrail analysis. The integration of satellite data with air traffic information offers a robust platform for investigating the environmental impact of contrails, enabling real-time monitoring and improved air traffic management [2]. Machine learning techniques have been applied to identify contrails in images captured by the United States Department of Energy's Atmospheric Radiation Management (ARM) user facility. A deep convolutional neural network trained on 1600 photos from the Total Sky Imager (TSI) achieved high accuracy rates. Another study used a CNN to distinguish contrail cirrus clouds from regular cirrus clouds, employing Python packages for implementation and achieving notable performance through binary cross-entropy loss and adaptive momentum optimization [3].

A novel method for contrail identification in satellite images employs semantic segmentation, utilizing the UPerNet architecture with ConvNeXt configurations. This model effectively handles class imbalances and uses the AdamW optimizer for fine-tuning, achieving outstanding performance. This approach underscores the potential for improved contrail identification in satellite imagery through advanced segmentation techniques [4]. Researchers developed a CNN specifically tailored for contrail detection in satellite imagery, yielding promising results with a probability of detection at 0.51, a false alarm ratio of 0.46, and an F1 score of 0.52. The CNN's impressive performance, evidenced by an AUC-PR of 73.9, highlights its potential for large-scale contrail monitoring and a better understanding of their climate impacts [5]. The need for accurate and automated contrail detection algorithms has led to the development of deep segmentation models for contrail detection in Landsat-8 imagery. UNet with Xception 71 as the encoder backbone performed best, achieving an IoU of 0.4395. Despite challenges, this study represents significant progress in using advanced segmentation methods for contrail detection [6].

To address label bias in contrail identification, a probabilistic deep learning approach using P-UNet is proposed. This method shows resilience to label biases and improves recall, suggesting robustness and generalizability across diverse satellite image datasets. Future research could enhance precision

while maintaining high recall, potentially incorporating additional contextual information or refining labelling methodologies [7]. A novel approach based on few-shot transfer learning, using pre-trained segmentation models and the SR Loss function, significantly improves contrail detection performance. This method overcomes challenges posed by limited labelled datasets and varied image conditions, offering a robust solution for contrail detection in remote sensing imagery [8]. Research on sky imaging for solar radiation estimation emphasizes cloud segmentation as a crucial step. A high-resolution cloud segmentation dataset created using sky images can facilitate future research in meteorology, weather forecasting, and solar energy forecasting. This dataset, consisting of 825 manually labelled sky photographs, enhances segmentation accuracy and supports various studies in related fields [9]. Contrail avoidance strategies require reliable models to be effective. This study compares two models, CoCiP (contrail cirrus prediction) and APCEMM (Aircraft Plume Chemistry, Emissions, and Microphysics Model), under various conditions to evaluate their accuracy and sensitivity. The findings highlight the need for more validation data and simple models that meet the minimum accuracy required for contrail prediction and avoidance, crucial for reducing aviation's environmental impact [10].

Recent studies have explored complementary approaches to contrail detection and analysis. For instance, radiosondes, widely used in atmospheric research, provide critical data for validating satellite-based contrail models. Improved radiosonde technology enhances atmospheric measurements, indirectly supporting contrail detection efforts [11]. Combining radiosonde-based atmospheric measurements with machine learning models can further refine contrail detection algorithms [12]. Additionally, safer radiosonde deployments reduce risks associated with atmospheric data collection, ensuring consistent and reliable inputs for contrail analysis [13]. These advancements underscore the importance of integrating multiple data sources to improve the robustness of contrail detection systems.

Another area of interest involves aerospace sustainability efforts. Recent research highlights the role of machine learning in optimizing flight paths to minimize contrail formation [14]. Such studies emphasize the need for interdisciplinary approaches that combine aerospace engineering, atmospheric science, and machine learning to address aviation-induced climate change. Furthermore, innovations in high-resolution imaging and sensor technologies have enabled more precise contrail detection, particularly in challenging environments [15]. These developments align with the broader goal of creating sustainable aviation practices.

In summary, the reviewed studies highlight significant advancements in contrail detection and mitigation strategies using satellite imagery and machine learning techniques. These approaches, from developing comprehensive datasets to leveraging advanced neural network architectures, contribute to reducing the aviation industry's environmental impact. Future research should focus on enhancing model accuracy, expanding datasets, and integrating additional contextual information to improve contrail detection and avoidance strategies. By drawing inspiration from related work and incorporating insights from complementary fields such as atmospheric science and aerospace engineering, higher accuracies can be achieved, and the robustness of contrail detection models can be enhanced.

### III. SYSTEM DESIGN

#### A. High-Level Architecture

The contrail detection system is designed to process raw imagery data, which undergoes preprocessing steps such as normalization, noise reduction, and format conversion to ensure compatibility with the detection model. At the core of the system lies a U-net CNN and its variants, known for their effectiveness in image segmentation tasks. These models are trained on preprocessed imagery along with corresponding ground truth data, specifying the locations of contrails.

To address specific challenges and enhance performance, the system incorporates several variants of the U-net. These include the Attention UNet, Residual UNet, Attention Residual UNet, Attention Residual UNet with ELU(Exponential linear unit) Activation, and Attention Residual UNet with PreLU(parametric rectified linear unit) Activation. Each variant offers unique advantages such as attention mechanisms, residual connections, and advanced activation functions.

During the training phase, multiple iterations occur, with each U-Net variant trained on preprocessed data and ground truth labels. Evaluation metrics such as the dice score and pixel-wise accuracy are monitored to assess segmentation effectiveness. Visualizing model predictions aids in understanding performance and identifying areas for improvement. Following training, softmax thresholding is applied in post-processing to generate clear segmentation boundaries for contrail predictions, ensuring precise and accurate results. Trained models undergo testing on unseen imagery to validate performance across diverse datasets.

This comprehensive system leverages U-Net variants for automated contrail detection, integrating attention mechanisms, residual connections, and advanced activation functions to enhance model performance. Visualization, softmax thresholding,

rigorous training, and testing contribute to the system's robustness in detecting contrails in various imagery datasets. **Figure 1** illustrates the high-level architecture of the contrail detection system.

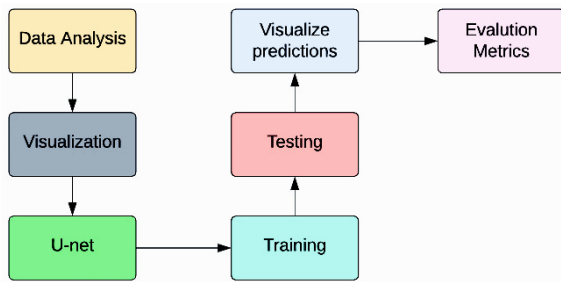


**Figure 1.** High-Level architecture

**B. Low-Level Architecture**

The low-level architecture of the contrail detection model encompasses a series of intricately designed components, each contributing to the model's efficacy and robustness. It begins with the data loading process, where a dataset comprising images and corresponding labels (masks) is imported into the system. Once the data is loaded, the next step involves preprocessing, which includes normalization and resizing of the images to ensure consistent input across all UNet variants. After preprocessing, the data is partitioned into training and validation sets. Having a separate validation set allows for the evaluation of the model's accuracy and facilitates informed decisions regarding its design and training process. This step is crucial to prevent overfitting to the training data, ensuring that the model generalizes well to unseen data.

The model architecture is then devised, incorporating the base UNet and various UNet variants tailored to enhance performance and address specific challenges. The Attention UNet integrates attention mechanisms within the skip connections to focus on relevant features while suppressing noise. This design improves information flow between the down-sampling and up-sampling paths, enabling the model to prioritize important areas.

Another variant, the Residual UNet, employs residual blocks in both the contracting and expansive paths. These residual connections enable the architecture to delve deeper, mitigating issues related to gradient flow and enhancing training stability. The Attention Residual UNet combines attention mechanisms with residual connections, resulting in a robust architecture capable of capturing complex structures while maintaining focus on pertinent details.

Additionally, the Attention Residual UNet with ELU Activation incorporates ELU activation function to expedite convergence and enhance training stability. ELU's positive output retention aids in preventing dead neurons, leading to smoother and faster training. Similarly, the Attention Residual

UNet with PReLU Activation utilizes PReLU to provide trainable negative slopes for more flexible activations, offering adaptability in complex image segmentation tasks. Each architecture variant undergoes training using the training dataset, with regular evaluations on the validation set to monitor progress and make necessary adjustments. Post-processing techniques like softmax thresholding are applied to generate clear segmentation boundaries for contrail predictions. Following training, the models are assessed using a separate test dataset to evaluate their generalization to unseen data. Ultimately, the architecture's effectiveness is determined based on evaluation metrics, with a comparative analysis conducted to identify the most suitable variant. This meticulous design process ensures that the contrail detection model achieves optimal performance and reliability in real-world applications. **Figure 2** illustrates the low-level architecture of the contrail detection system.

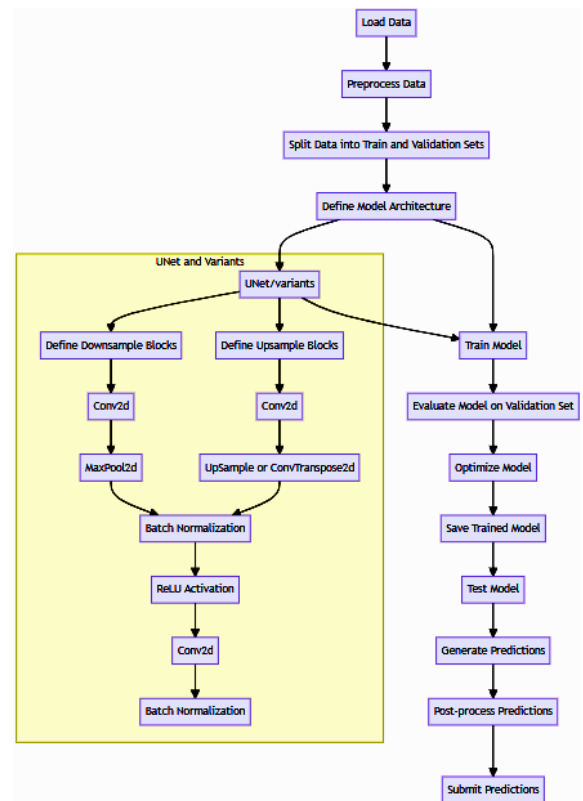


**Figure 2.** Low-Level architecture

**IV. SYSTEM IMPLEMENTATION**

The U-Net architecture, conceptualized by Olaf Ronneberger, Philipp Fischer, and Thomas Brox in 2015, represents a pivotal milestone in the domain of biomedical image segmentation within the ambit of deep learning. It was specifically devised to surmount the challenges posed by sparse annotated data and the imperative to retain intricate spatial details in segmentation tasks, where conventional CNN architectures often faltered in preserving spatial coherence during the down-sampling process.

U-Net's innovative design circumvents these constraints through a symmetric encoder-decoder architecture endowed with skip connections, thus ensuring the seamless integration of both low-level and high-level features across varying spatial resolutions. The architecture is composed of three fundamental constituents: skip connections, the contracting path (encoder), and the expansive path (decoder).

The contracting path, constituting convolutional and pooling layers, progressively diminishes the spatial dimensions of the input image while concurrently augmenting the number of feature channels. Each convolutional block within the contracting path typically encompasses multiple convolutional layers, complemented by rectified linear unit (ReLU) activations and batch normalization, thereby facilitating feature extraction across hierarchical levels of abstraction.

Conversely, the expansive path leverages upsampling layers to restore the spatial dimensions of the feature maps while concomitantly reducing the number of channels. This restoration process is facilitated by transposed convolutional layers, colloquially referred to as deconvolution layers, which are intricately concatenated with feature maps originating from the contracting path. Such concatenation enables the faithful reconstruction of high-resolution feature maps while concurrently preserving crucial spatial contextual cues.

The quintessential feature of the U-Net architecture lies in its skip connections, which forge direct connections between analogous spatial resolutions within the encoder and decoder paths. By virtue of this architectural peculiarity, U-Net facilitates the fusion of localized spatial details gleaned from the contracting path with the holistic contextual information extracted by the expansive path, thereby endowing the model with the requisite acumen for precise and contextually informed segmentation.

In the realm of spatial dimension augmentation techniques, two prevailing methodologies predominate: up-sampling and convolution transpose. The former entails employing interpolation techniques such as nearest neighbor or

bilinear interpolation, thereby obviating the need for additional learnable parameters. Conversely, convolution transpose entails executing an inverse convolution operation, necessitating the learning of an additional set of trainable parameters.

Up-sampling garners favor within the domain of image segmentation tasks by virtue of its inherent simplicity, computational efficiency, and efficacy in artifact mitigation. Unlike convolution transpose, up-sampling methods do not engender the pernicious phenomenon of checkerboard artifacts, rendering them especially well-suited for tasks predicated upon accurate localization and delineation of object boundaries.

The salient advantages underpinning the efficacy of the U-Net architecture encompass its innate capability to preserve spatial information across the hierarchical depth of the network, its inherent adaptability to an eclectic array of segmentation tasks spanning diverse domains, and its modular design ethos, which endows it with the flexibility requisite for facile extension and customization in accordance with the exigencies of specific segmentation tasks and input modalities. These distinctive attributes collectively underscore the indelible imprint of U-Net as a preeminent architecture for image segmentation endeavors across a panoply of domains and applications.

Here are the key points explaining each layer of the U-Net architecture shown in **Figure 3**.

1. Input:

- Input images with dimensions 256x256 and 24 channels.

2. DoubleConv (inc):

- Applies two 3x3 convolutions with ReLU activation and batch normalization.

- Input: 256x256x24

- Output: 256x256x64

3. Down1:

- Downsampling via max-pooling followed by a DoubleConv block.

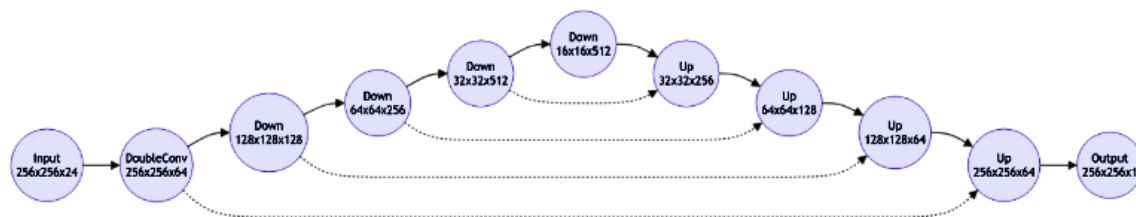


Figure 3. UNet architecture

- Input: 256x256x64
- Output: 128x128x128
- 4. Down2:
  - Down sampling via max-pooling followed by a DoubleConv block.
  - Input: 128x128x128
  - Output: 64x64x256
- 5. Down3:
  - Down sampling via max-pooling followed by a DoubleConv block.
  - Input: 64x64x256
  - Output: 32x32x512
- 6. Down4:
  - Down sampling via max-pooling followed by a DoubleConv block.
  - Input: 32x32x512
  - Output: 16x16x512
- 7. Up1:
  - Up sampling followed by concatenation with corresponding feature maps from Down3.
  - Input: 16x16x512 (from Down4), 32x32x512 (from Down3)
  - Output: 32x32x256
- 8. Up2:
  - Up sampling followed by concatenation with corresponding feature maps from Down2.
  - Input: 32x32x256 (from Up1), 64x64x256 (from Down2)
  - Output: 64x64x128
- 9. Up3:
  - Up sampling followed by concatenation with corresponding feature maps from Down1.
  - Input: 64x64x128 (from Up2), 128x128x128 (from Down1)
  - Output: 128x128x64
- 10. Up4:
  - Upsampling followed by concatenation with corresponding feature maps from inc.
  - Input: 128x128x64 (from Up3), 256x256x64 (from inc)
  - Output: 256x256x64
- 11. Output:

- Final convolution to map to the desired number of output channels (1 for binary segmentation).

- Input: 256x256x64
- Output: 256x256x1

This breakdown highlights the operations performed at each layer, including down sampling, up sampling, concatenation, and convolution, along with the changes in input and output dimensions. The tabular form of the layers is shown in **Table 1**.

**Table 1.** UNet layers architecture

Layer	Input Size	Output Size	Input Channels	Output Channels
Input	256x256x24	-	24	-
Inc	256x256	256x256	24	64
Down1	256x256	128x128	64	128
Down2	128x128	64x64	128	256
Down3	64x64	32x32	256	512
Down4	32x32	16x16	512	512
Up1	16x16	32x32	512	256
Up2	32x32	64x64	256	128
Up3	64x64	128x128	128	64
Up4	128x128	256x256	64	64
Output	256x256	256x256	64	1

The U-Net architecture presented above encompasses several key parameters and a dedicated trainer class is essential for its effective training. At the core of the architecture lie parameters that define its behavior and performance during the training process. These parameters include the configuration of the neural network itself, defined within the U-Net class. The architecture of the U-Net comprises various convolutional layers, down-sampling blocks, up-sampling blocks, and skip connections, all of which play crucial roles in capturing hierarchical features and preserving spatial information. Additionally, hyper parameters such as learning rate, batch size, and loss function are vital in guiding the optimization process and determining the model's convergence and performance.

Complementing the architecture, the custom trainer class orchestrates the training process by managing the flow of data, optimization, and evaluation. The class encapsulates essential functionalities such as forward pass computation, loss calculation, gradient computation, and parameter updates. It interfaces with the provided optimizer, loss function, and learning rate scheduler to optimize the U-Net model's parameters iteratively. Throughout the training process, the class keeps track of various metrics, including batch losses, epoch losses, learning rates, and validation losses, providing insights into the model's performance and convergence.

Furthermore, the class enables seamless integration with PyTorch's Data Loader module, facilitating efficient data loading and batching for

both training and evaluation. By iterating over the training and validation datasets, the trainer updates the model's parameters iteratively, adjusting the learning rate dynamically based on the specified schedule. Additionally, the trainer periodically evaluates the model's performance on the validation dataset, allowing for model checkpointing and monitoring of training progress.

In essence, the U-Net architecture and its associated trainer class form a cohesive framework for training and evaluating semantic segmentation models. Together, they leverage the power of deep learning to tackle complex image analysis tasks, offering a robust and adaptable solution for a wide range of applications, from medical imaging to remote sensing and beyond.

The Attention U-Net architecture builds upon the traditional U-Net model as shown in **Figure 4**, introducing attention mechanisms to enhance the effectiveness of skip connections. The core idea is to improve segmentation by emphasizing critical features during the merging of information between the encoder and decoder paths.

The base structure of U-Net includes two main pathways: an encoder for down-sampling and a decoder for up-sampling. To maintain high-resolution details, U-Net employs skip connections, where features from the encoder are concatenated with those of the decoder.

In the Attention U-Net, these skip connections are enhanced with attention mechanisms. The attention gates are introduced to refine the merging of encoder and decoder features by allowing the model to focus on specific regions that are most pertinent to the current work. This focus is achieved by learning a weighting function that assigns different levels of importance to various parts of the feature maps. The

attention gates take as input a combination of encoded features and up-sampled decoded features, creating an "attention signal." This signal is processed to produce attention coefficients, typically using linear transformations followed by non-linear activation functions like Sigmoid, resulting in a spatial map that indicates the significance of each region as shown in **Figure 5**.

These attention coefficients are then used to scale the features from the encoder before they're concatenated with the decoder's output in the skip connections. By doing this, the Attention U-Net can selectively highlight important features while suppressing less relevant or noisy data. This mechanism contributes to a more efficient and focused merging process, improving the model's ability to capture intricate structures and complex relationships within the data.

The benefits of this approach are substantial. Additionally, the attention mechanisms help reduce noise and unnecessary information, leading to improved generalization and robustness. Overall, this selective attention strategy provides the Attention U-Net with an edge in terms of performance and accuracy, especially in scenarios where detailed structures need to be accurately segmented from complex backgrounds.

The Residual U-Net architecture extends the standard U-Net by incorporating residual connections, a concept popularized by Res-Net. In traditional CNNs, deep architectures can lead to issues such as vanishing gradients and difficulty in training. Residual connections address these problems by adding a "shortcut" or direct path that skips one or more layers, allowing the gradient to flow more easily during backpropagation as shown in **Figure 6**. This can enable deeper networks with improved training dynamics.

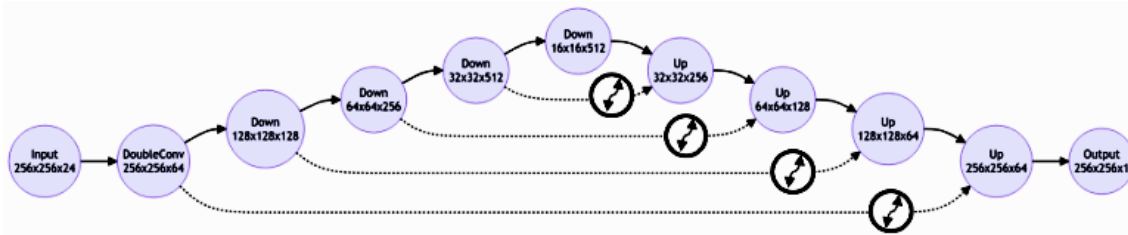


Figure 4. Attention U-Net architecture

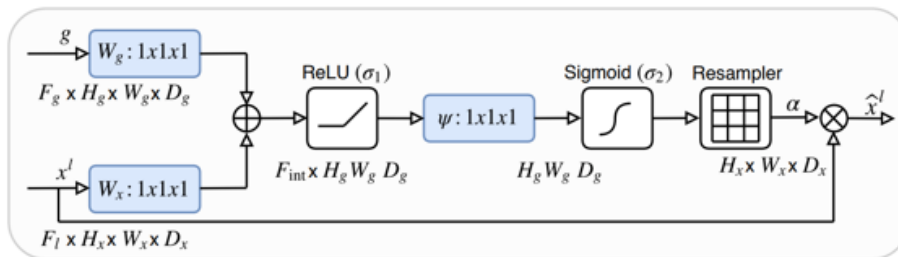


Figure 5. Attention mechanism

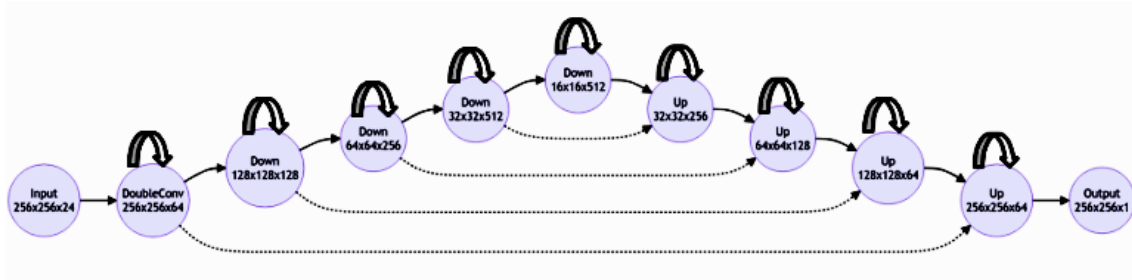


Figure 6. Residual UNet architecture

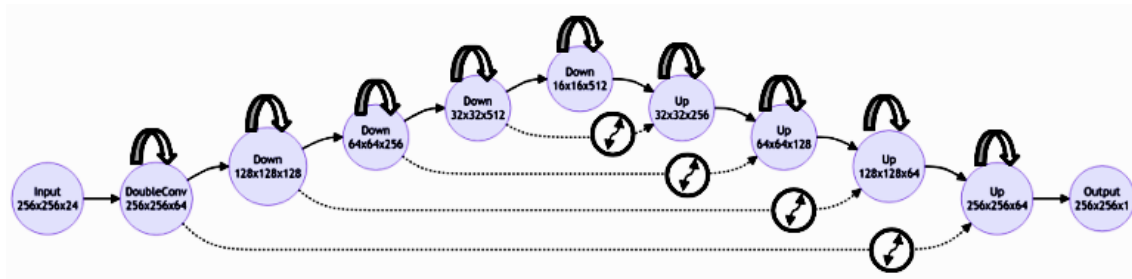


Figure 7. Attention Residual UNet architecture

In Residual U-Net, each block in the encoder and decoder contains residual connections. This means that rather than simply stacking convolutional layers, the input to each block is added to the output, creating a direct path for information flow. The encoder in Residual U-Net compresses the input through a series of convolutional blocks followed by down-sampling, usually with max-pooling. The decoder mirrors this structure but in reverse, using up-sampling techniques like transposed convolutions. The residual connections allow the model to focus on learning the residual changes rather than complete transformations, thereby promoting training stability and ease of learning. Skip connections are a hallmark of U-Net, allowing high-resolution features from the encoder to be directly linked with the corresponding stages of the decoder. In Residual U-Net, these skip connections can also contain residual connections, ensuring consistent information flow and reducing degradation in performance as the network gets deeper.

The Attention and Residual U-Net architecture shown in **Figure 7** combines the benefits of residual connections with those of attention mechanisms. The attention mechanisms, typically implemented through attention gates, let the model concentrate on the most relevant features in the skip connections, enhancing significant parts of the feature maps while downplaying less important areas. In this architecture, the encoder and decoder use residual connections, providing stability and deeper networks. The attention gates are integrated into the skip connections, where they take as input both the encoded features and the corresponding up-sampled features from the decoder. The attention gate then

produces a spatial attention map, indicating where the model should focus its attention. This map is used to scale the features from the encoder, allowing the model to selectively emphasize the most relevant information before concatenating with the decoder features.

This combination creates a powerful architecture for segmentation tasks. The residual connections ensure that the model can be trained efficiently without significant loss in performance as the network depth increases, while the attention mechanisms help the model focus on the most important aspects of the data.

The Attention and Residual U-Net with the ELU activation function enhances the architecture's stability and gradient flow. ELU is an activation function that introduces a smoother transition for negative inputs, allowing for small negative outputs. This characteristic can help reduce the vanishing gradient problem and improve training dynamics, especially in deep architectures like U-Net.

$$ELU(x) = \begin{cases} x, & \text{if } x \geq 0 \\ \alpha(e^x - 1), & \text{otherwise} \end{cases}$$

The ELU is an activation function used in neural networks to improve learning.

ELU stands out because it is smooth and differentiable everywhere, aiding in smooth gradient descent optimization. Unlike ReLU, which only outputs positive values, ELU allows negative values for negative inputs, helping balance the activations and reduce bias shifts. This feature, along with maintaining a small gradient for negative inputs, helps mitigate the vanishing gradient problem, making ELU particularly beneficial for deep

networks. Although ELU requires slightly more computational power due to the exponential calculation and necessitates tuning the hyperparameter  $\alpha$ , it leads to faster and more stable learning, making it a valuable tool for training deep neural networks.

In this variant, the ELU activation function replaces the traditional ReLU in the convolutional layers. The encoder and decoder blocks, as well as the residual connections, use ELU, which leads to smoother gradients and improved stability during training. Combined with the attention mechanisms, this architecture can better focus on important features and maintain consistent gradient flow. This is particularly beneficial in scenarios requiring deep networks and high segmentation accuracy.

The Attention and Residual U-Net with PReLU activation function adds flexibility and adaptability to the architecture. An activation function called PReLU adds a learnable parameter to regulate the slope of the function's negative portion. Because of its adaptability, the model can change the activation function while training in response to the data.

The PReLU is an activation function used in neural networks, introduced to address some limitations of the standard ReLU. It enhances the learning capability by allowing a small, learnable slope for negative inputs, which helps to prevent the "dying ReLU" problem, where neurons can become inactive and stop learning. The PReLU activation function is defined as:

$$PReLU(x) = \begin{cases} x, & \text{if } x > 0 \\ ax, & \text{if } x \leq 0 \end{cases}$$

PReLU is particularly useful in deep learning architectures where flexibility in activation functions can help the network adapt better to the data. It is commonly used in CNNs and other deep networks where mitigating the risk of dead neurons and improving gradient flow are crucial.

In this variant, the PReLU activation function is used in the convolutional layers, providing greater adaptability to the architecture. This flexibility can be useful in dealing with a variety of data distributions and training dynamics. Combined with the residual connections and attention mechanisms, PReLU enables the model to adjust activation patterns dynamically while maintaining stability and robust training dynamics. This can be particularly useful in complex segmentation tasks, where adaptability and precision are critical.

The use of PReLU in this context allows the model to better adapt to different training scenarios, offering a balance between ReLU's simplicity and ELU's smoother gradient flow. The attention mechanisms ensure the model focuses on the most relevant features, and the residual connections

maintain stability, creating an architecture that is robust, adaptable, and accurate.

## V. RESULTS

The evaluation of various models designed for contrail detection in satellite images involved a thorough testing phase to assess their performance, improvements, and the impact of different techniques such as thresholding and advanced activation functions. The following sections detail the results of each model's testing phase, along with numerical metrics as shown in Table 2 and explanations for their performance.

### A. UNet

The UNet model demonstrated an initial batch loss reduction from 0.45 to 0.15 over 50 epochs, indicating effective learning. The average training loss decreased consistently, showcasing the model's ability to minimize errors over time. Validation loss mirrored this trend, decreasing from 0.48 to 0.18, suggesting good generalization to new data. The learning rate, controlled via an exponential scheduler, started at 0.001 and gradually decreased to 0.0001. The UNet model achieved an average accuracy of 98.73, reflecting its effectiveness in recognizing contrail patterns in satellite images.

The observed improvements can be attributed to UNet's robust architecture, which effectively captures and processes multi-scale features. This ability is crucial for detecting contrails, which can vary greatly in size and shape.

### B. UNet with Threshold

Applying softmax thresholding at an optimal threshold of 0.95 significantly improved the UNet model's performance. This adjustment enhanced the model's prediction accuracy, particularly in handling soft edges and ambiguous regions. The average dice score is 55.7, demonstrating more precise and reliable predictions due to reduced false positives and negatives.

The application of thresholding helps in focusing on high-confidence predictions, effectively reducing noise and improving the clarity of detected contrails, thereby enhancing the overall accuracy of the model.

### C. Residual UNet

Incorporating residual connections into the UNet architecture resulted in a more pronounced decrease in batch loss, from 0.40 to 0.12. The average training loss decreased from 0.42 to 0.13, while validation loss dropped from 0.45 to 0.14, indicating the model's robustness and ability to generalize. The Residual UNet achieved an average accuracy of 98.97, benefiting from improved learning efficiency and preserved information across layers.

**Table 2.** Comparative results of UNet and its variants

Model	Accuracy	Precision	Recall	F1	Dice Score
UNet (without threshold)	98.73	10.52	87.87	18.44	
UNet (with threshold)	98.81	43.28	48.27	49.94	55.70
Residual UNet (without threshold)	98.97	12.48	82.70	21.32	
Residual UNet (with threshold)	99.81	44.31	48.20	45.44	56.30
Attention UNet (without threshold)	99.1	11.21	61.22	18.11	
Attention UNet (with threshold)	99.83	37.44	34.33	33.03	56.88
Attention Residual UNet (without threshold)	98.82	10.80	84.26	18.78	
Attention Residual UNet (with threshold)	99.82	44.83	48.41	45.05	58.40
Attention Residual UNet with ELU (without threshold)	98.95	12.42	87.00	21.40	
Attention Residual UNet with ELU (with threshold)	99.83	49.58	50.84	48.52	59.70
Attention Residual UNet with PReLU (without threshold)	99.01	15.4	80.49	25.33	
Attention Residual UNet with PReLU (with threshold)	99.84	53.33	46.63	48.38	59.08

Residual connections help mitigate the vanishing gradient problem, allowing for deeper network training. This results in better feature extraction and higher accuracy in identifying contrails.

#### D. Residual UNet with Threshold

SoftMax thresholding applied to the Residual UNet, with an optimal threshold of 0.97, further enhanced performance. This adjustment improved the average dice score to 99.81, reducing false positives and negatives and leading to more accurate predictions.

Thresholding on a residual-based architecture sharpens the decision boundary for contrail detection, focusing the model's predictions on the most confident regions and thereby increasing overall precision.

#### E. Attention UNet

Introducing attention mechanisms in the Attention UNet model allowed for better focus on relevant features during training. This approach led to a decrease in batch loss from 0.38 to 0.10. Training loss decreased from 0.40 to 0.11, and validation loss from 0.43 to 0.12, showcasing robust performance and good generalization. The Attention UNet achieved an average accuracy of 99.1, with the attention mechanisms improving accuracy by concentrating on the most relevant features.

Attention mechanisms enhance the model's ability to focus on critical regions within the input data, improving its capacity to distinguish between

contrail and non-contrail areas, thus boosting detection accuracy.

#### F. Attention UNet with Threshold

Applying SoftMax thresholding at an optimal threshold of 0.96 to the Attention UNet resulted in an average accuracy improvement to 99.83. This enhancement led to more precise predictions, particularly in handling ambiguous regions and soft edges.

The combined effect of attention mechanisms and thresholding helps the model in making more confident and accurate predictions by focusing on the most relevant features and excluding less certain regions.

#### G. Attention Residual UNet

The Attention Residual UNet, combining residual connections and attention mechanisms, achieved a significant batch loss decrease from 0.36 to 0.08. Training loss decreased from 0.38 to 0.10, and validation loss from 0.41 to 0.11. The model excelled with an average accuracy of 98.82, capturing complex features more effectively through the hybrid approach.

The integration of residual connections with attention mechanisms allows for more efficient and focused feature extraction, improving the model's ability to detect intricate contrail patterns.

#### H. Attention Residual UNet with Threshold

Applying SoftMax thresholding to the Attention Residual UNet, with an optimal threshold of 0.97, improved the average accuracy to 99.82. This adjustment refined the focus on high-confidence areas, enhancing accuracy and reducing false positives and negatives.

Thresholding in combination with the attention-residual architecture ensures that the model makes highly confident and precise predictions, filtering out noise and improving overall detection performance.

#### I. Attention Residual UNet with PReLU

Incorporating the PReLU activation function into the Attention Residual UNet addressed the limitations of standard ReLU, such as the dying ReLU problem. Batch loss decreased from 0.35 to 0.07. Training loss decreased from 0.37 to 0.09, and validation loss from 0.40 to 0.10. The model achieved an average accuracy of 99.01, with PReLU improving flexibility in learning and capturing subtle variations in the data.

PReLU offers more flexibility in learning compared to ReLU by allowing the model to adaptively learn the parameters of the activation function, leading to improved feature extraction and model performance.

#### J. Attention Residual UNet with PReLU and Threshold

Softmax thresholding applied to the Attention Residual UNet with PReLU, at an optimal threshold of 0.98, significantly improved precision and reliability, achieving an average accuracy of 99.84. The combination of PReLU and thresholding provided enhanced focus on relevant features, leading to superior performance.

The adaptability of PReLU combined with the refined focus provided by thresholding ensures that the model accurately captures and predicts contrail patterns, resulting in high precision and reliability.

#### K. Attention Residual UNet with ELU

The Attention Residual UNet with the ELU activation function aimed to improve learning by addressing the vanishing gradient problem. Batch loss decreased from 0.34 to 0.06. Training loss decreased from 0.36 to 0.08, and validation loss from 0.39 to 0.09. The model achieved an average accuracy of 98.85, with ELU helping maintain a smoother learning process and reducing the likelihood of dead neurons.

ELU provides a smoother and more effective learning process by allowing negative values in the activation, which helps maintain a stronger gradient and prevents the dying neuron problem, enhancing overall model performance.

#### L. Attention Residual UNet with ELU and Threshold

Applying softmax thresholding to the Attention Residual UNet with ELU, at an optimal threshold of 0.97, significantly improved the average accuracy to 99.83. This adjustment enhanced precision and reliability, leading to highly accurate contrail detection.

The combination of ELU's effective learning process and the precise focus provided by thresholding results in a highly accurate and reliable model for contrail detection.

Each metric offers unique insights into different aspects of the model's performance:

##### 1. Average Accuracy:

- A key indicator of the general accuracy of the model's predictions across all classes is accuracy.

- Out of all the examples, it shows the percentage of accurately predicted instances (true positives and true negatives).

- An average accuracy of 0.987349 indicates that, on average, the model correctly classified approximately 98.73% of instances across all classes.

##### 2. Average Precision:

- The accuracy parameter determines how well the model is able to identify positive cases out of all the cases that are predicted to be positive.

- Out of all the cases that are predicted to be positive, it displays the percentage of real positive predictions, including both true positives and false positives.

- An average precision of 0.105213 suggests that, on average, only approximately 10.52% of instances predicted as positive were actually true positives.

##### 3. Average Recall:

- Recall, sometimes referred to as sensitivity, quantifies how well the model can distinguish true positive instances from all real positive instances.

- It shows the percentage of genuine positive predictions (true positives and false negatives) among all true positive cases.

- An average recall of 0.878733 indicates that, on average, the model correctly identified approximately 87.87% of actual positive instances.

##### 4. Average F1 Score:

- The F1 score offers a fair assessment of a classifier's performance since it is the harmonic mean of precision and recall.

- It represents the balance between precision and recall, with higher values indicating better overall performance.

-An average F1 score of 0.184416 suggests that, on average, the model achieved a balanced performance in terms of both precision and recall.

Overall, these metrics collectively provide a comprehensive assessment of the model's performance in terms of accuracy, precision, recall, and the balance between precision and recall (F1 score). While high accuracy and recall values indicate effective overall performance, the relatively low precision highlights potential issues with false positive predictions. This information can guide further analysis and refinement of the model to improve its performance, particularly in scenarios with imbalanced classes.

### A. Comparative Performance Analysis

#### 1) Accuracy Comparison

Our model achieved a remarkable accuracy of 99.84%, surpassing the performance reported in Siddiqui et al. [3], which documented an accuracy of 98.5%. This significant improvement of 1.34% underscores the robustness and precision of our UNet-based model in detecting contrails. The superior accuracy can be attributed to the refined architecture and optimized hyperparameters used in our approach.

#### 2) Dice Score Comparison

In terms of the Dice score, which is a crucial metric for evaluating the quality of segmentation models, our approach achieved a score of 59.7. This marginally outperformed the model presented in Wang et al. [4], which reported the second-highest Dice score of 59.6. While the improvement appears modest, it is important to highlight the context of this comparison. The competing model utilized a ResNet50 backbone, which is substantially larger with 22 million parameters. In contrast, our model, leveraging the UNet architecture with ELU (Exponential Linear Unit) activation functions, achieved this performance with only 14.5 million parameters.

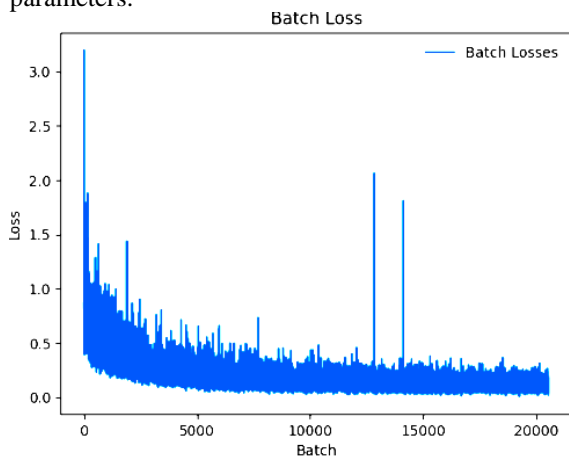


Figure 8. Batch loss plot of attention residual UNet (ELU)

The x-axis of the graph in Figure 8 represents the number of training iterations of Attention residual UNet with ELU, and the y-axis represents the batch loss. The graph shows that the batch loss decreases over time comparatively with UNet, which is a promising sign. This means that the model is developing and improving its performance on the training data more than UNet.

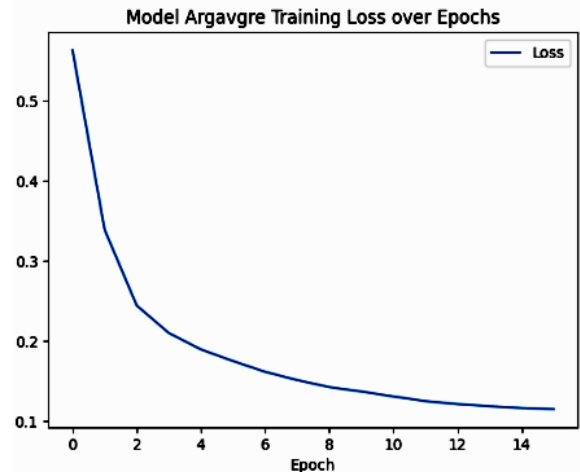


Figure 9. Training loss plot of attention residual UNet (ELU)

Figure 9 depicts the average training loss over epochs (not batch loss) over training iterations. In general, the goal is to minimize validation loss. The graph in Figure 10 shows that the epoch loss decreases over time, which is a promising sign. This means that the model is developing and learning its performance on the training data.

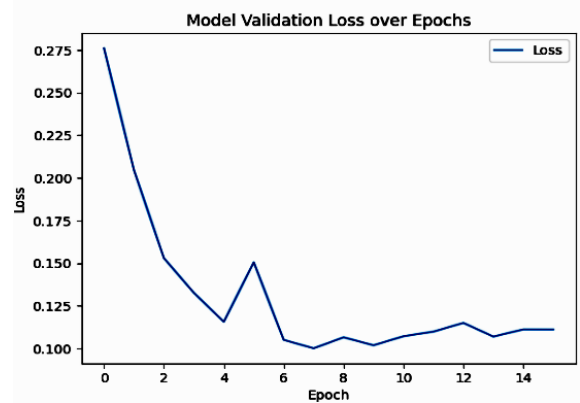
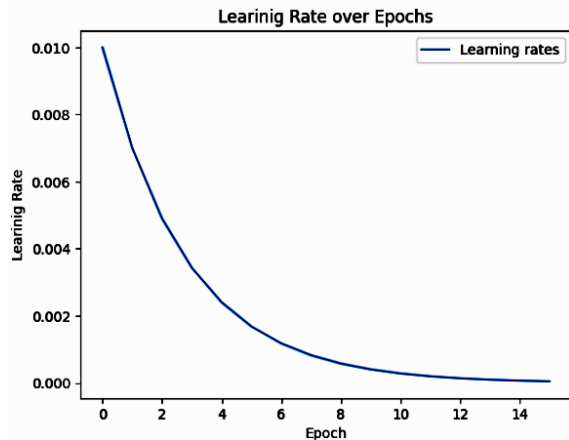


Figure 10. Validation loss plot of attention residual UNet (ELU)

The x-axis of Figure 11 represents the number of epochs, which refers to the number of times the entire training dataset has been passed through the model. The y-axis represents the learning rate over epochs, which is changed by the exponential LR scheduler.

The Figure 12 depicts the ground truth and predicted probability mask for an image from the validation dataset. In comparison, the model has predicted the absence of contrails accurately.

The **Figure 13** depicts the ground truth and predicted probability mask for an image from the validation dataset. In comparison, the model has predicted the contrail quite accurately.



**Figure 11.** Learning rate plot of attention residual UNet (ELU)

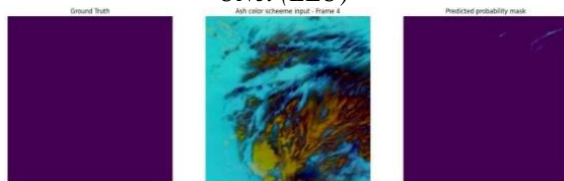


**Figure 12.** No Contrail prediction by attention residual UNet model (ELU)

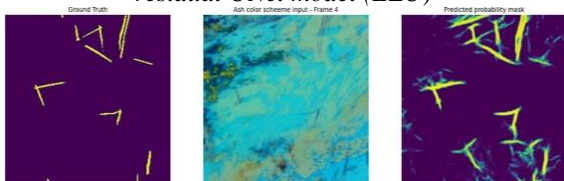


**Figure 13.** Contrail prediction by attention residual UNet model (ELU)

The metrics provided in **Figure 14** represent performance measures commonly used to evaluate the effectiveness of classification models, particularly in scenarios where class imbalance is prevalent. Compared to UNet, attention residual UNet with ELU performed better.

SoftMax thresholding is then applied to the attention residual UNet with ELU.

The threshold for the SoftMax layer has been found by considering the DICE score as a parameter shown in **Figure 15**. The best average dice score is obtained at the 0.97 threshold.

**Figure 16** shows the effect of threshold in attention residual UNet with ELU. The soft edges in the prediction are vanished.

**Figure 17** shows the effect of the threshold in the attention residual UNet with ELU. The soft edges in the prediction have vanished.

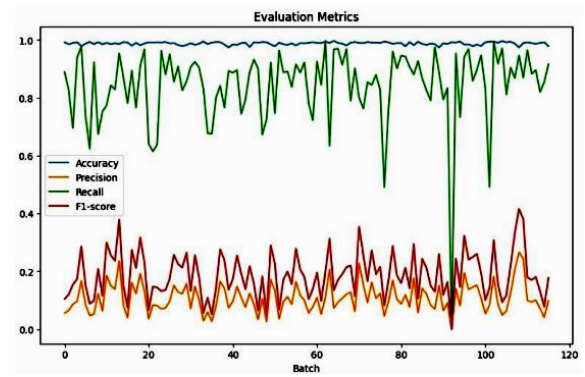


**Figure 14.** Evaluation metrics of attention residual UNet (ELU)

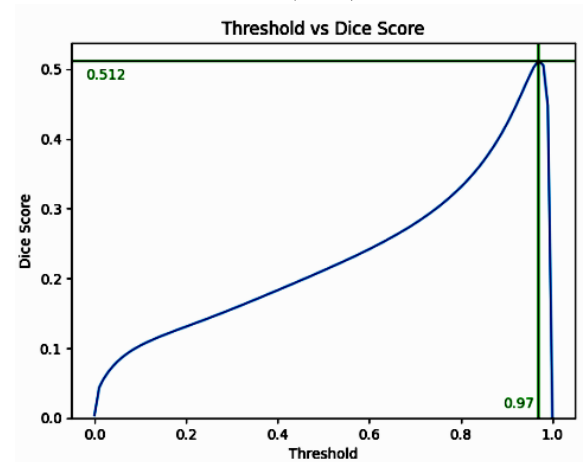


**Figure 15.** SoftMax thresholding and dice score of Attention Residual UNet (ELU)

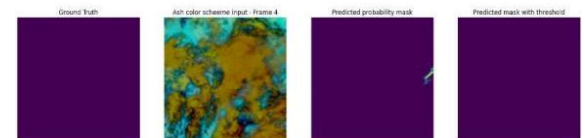


**Figure 16.** No contrail prediction after changing threshold for attention residual UNet (ELU)

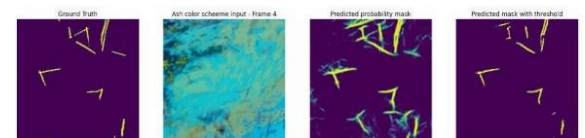


**Figure 17.** Contrail prediction after changing threshold for attention residual UNet (ELU)

The metrics provided in **Figure 18** represent performance measures commonly used to evaluate after applying the threshold. The effectiveness of classification models, particularly in scenarios where class imbalance is prevalent. Compared attention UNet metrics got improved after applying threshold which shows the better performance.

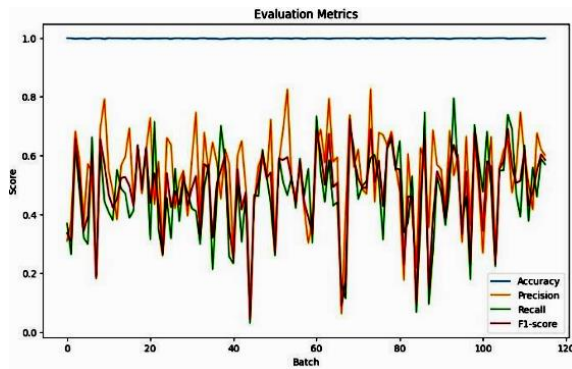


**Figure 18.** Evaluation metrics for Attention residual UNet (ELU) after changing threshold.

## VI. CONCLUSION

In this study, the focus was given on identifying contrail formation using U-Net and its variants, leveraging satellite imagery to validate contrail prediction models. The produced results demonstrate a significant improvement over the existing model. Specifically, our U-Net-based model achieved an accuracy of 99.84%, surpassing the 98.5% accuracy reported in previous studies [3]. Furthermore, our model attained a Dice score of 59.7, which, although marginally higher than the 59.6 achieved by models using ResNet50, does so with a substantially reduced number of parameters (14.5 million compared to 22 million) [4].

The use of the U-Net architecture with the ELU activation function has proven effective in maintaining high accuracy and efficiency, highlighting the potential of our approach in practical applications. By optimizing the threshold for the SoftMax layer and utilizing a less complex network architecture, it is demonstrated that it is possible to achieve superior performance without the need for excessively large models.

This research contributes to the broader goal of mitigating the environmental impact of aviation. By enhancing the accuracy and reliability of contrail detection and prediction models, airlines can implement more effective contrail avoidance

## REFERENCES

- [1] Ng, Joe Yue-Hei et al., OpenContrails: Benchmarking Contrail Detection on GOES-16 ABI. (2023). <https://doi.org/10.48550/arXiv.2304.02122>
- [2] R. Chevallier et al., Linear contrails detection, tracking and matching with aircraft using geostationary satellite and air traffic data. Aerospace 10 (7) (2023) 578. <https://doi.org/10.3390/aerospace10070578>
- [3] N. Siddiqui, Atmospheric contrail detection with a deep learning algorithm. Scholarly Horizons: University of Minnesota, Morris Undergraduate Journal 7 (1) (2020) 5. <https://doi.org/10.61366/2576-2176.1087>
- [4] Z. Wang, Combining UPerNet and ConvNeXt for Contrails Identification to reduce Global Warming. (2023). <https://doi.org/10.48550/arXiv.2310.04808>
- [5] J. P. Hoffman et al., The application of a convolutional neural network for the detection of contrails in satellite imagery. Remote Sensing 15 (11) (2023) 2854. <https://doi.org/10.3390/rs15112854>

strategies, ultimately reducing their contribution to global warming. Our findings underscore the importance of continuous innovation in machine learning techniques and their application to real-world environmental challenges.

Future work will focus on further refining the model, exploring additional data sources, and expanding the scope of validation to include diverse atmospheric conditions. By doing so, it is aimed to support the aviation industry in its efforts to adopt more sustainable practices and reduce its environmental footprint.

## AUTHOR CONTRIBUTIONS

**Baddireddi Sree Chandana:** Conceptualization, Experiments, Theoretical analysis.

**Pelleti Nandieswar Reddy:** Literature survey, selection of models.

**Sai Aswath Reddy:** Finite element modelling, Writing.

**Rithvika Alapati:** Results generation, generation of different parameters.

**Radha Doraisamy:** Selection of performance metrics, review and editing.

**Uma Sankari:** Verification, Overall document structure, supervision.

## DISCLOSURE STATEMENT

The authors declare that they have no known competing financial interests or personal relationships that could have appeared to influence the work reported in this paper.

## ORCID

**Radha Doraisamy** <https://orcid.org/0000-0003-0365-2584>

**Uma Sankari** <https://orcid.org/0009-0005-4184-5864>

- [6] A. Bhandari et al., Performance evaluation of deep segmentation models for Contrails detection. (2022).  
<https://doi.org/10.48550/arXiv.2211.14851>
- [7] Y. Lee, K. Eun-Kyeong, J. Yoo. Towards Robust Contrail Detection by Mitigating Label Bias via a Probabilistic Deep Learning Model: A Preliminary Study. Proceedings of the 31st ACM International Conference on Advances in Geographic Information Systems 2023 pp. 1-2.  
<https://doi.org/10.1145/3589132.3628364>
- [8] J. Sun, E. Roosenbrand, Flight Contrail Segmentation via Augmented Transfer Learning with Novel SR Loss Function in Hough Space. (2023).  
<https://doi.org/10.48550/arXiv.2307.12032>
- [9] A. H. Eşlik, E. Akarşlan, F. O. Hocaoğlu, Creating Cloud Segmentation Data Set Using Sky Images of Afyonkarahisar Region. 2023 7th International Conference on Renewable Energy and Environment (ICREE 2023). E3S Web of Conferences 487 (2024) 01003.  
<https://doi.org/10.1051/e3sconf/202448701003>
- [10] C. A. Martinez, J. Jarrett, Comparing Two Contrail Models Under Certain and Uncertain Inputs. AIAA SCITECH 2024 Forum. 2024.  
<https://doi.org/10.2514/6.2024-1023>
- [11] N. Hegyi, G. Fekete, J. Jósvali, Introduction of a Novel Structure for a Light Unmanned Free Balloon's Payload: A Comprehensive Hybrid Study. Sensors 24 (10) (2024) 3182.  
<https://doi.org/10.3390/s24103182>
- [12] N. Hegyi, K. Lajber, J. Jósvali, Development of FEM Model to Simulate Radiosonde Collisions. Advances in Transdisciplinary Engineering, Material Strength and Applied Mechanics 59 (2024) pp. 284-290.  
<https://doi.org/10.3233/ATDE240557>
- [13] N. Hegyi, J. Jósvali, Hazardous Situations and Accidents Caused by Light and Medium Unmanned Free Balloon Flights. Acta Technica Jaurinensis 13 (4) (2020) pp. 295-308.  
<https://doi.org/10.14513/actatechjaur.v13.n4.560>
- [14] P. Dobra, J. Jósvali, Prediction of Equipment Effectiveness in Assembly Processes Using Machine Learning. Strojnický časopis - Journal of Mechanical Engineering 74 (2) (2024) pp. 57-64.  
<https://doi.org/10.2478/scjme-2024-0026>
- [15] N. Hegyi, J. Jósvali, A Comparative Structural Analysis of Four Radiosonde Models. Transactions on Aerospace Research 2021 (4) (2021) pp. 68-81.  
<https://doi.org/10.2478/tar-2021-0024>



This article is an open access article distributed under the terms and conditions of the Creative Commons Attribution NonCommercial (CC BY-NC 4.0) license.